Materials Transactions, Vol. 46, No. 6 (2005) pp. 1230 to 1234
Special Issue on Computer Modeling of Materials and Processes

Experimental and Computational Investigation of Formation of Precipitate Free Zones in an Al–Cu Alloy

Shoichi Hirosawa, Yoshifumi Oguri* and Tatsuo Sato

Department of Metallurgy and Ceramics Science, Tokyo Institute of Technology, Tokyo 152-8552, Japan

Formation mechanisms of precipitate free zones (PFZ) in an artificially aged Al–1.74 mol%Cu alloy have been clarified using transmission electron microscopy (TEM), energy dispersive X-ray spectroscopy (EDX) and a Monte Carlo computer simulation. The vacancy depletion mechanism caused by the annihilation of quenched-in excess vacancies was found to work predominantly in the early stage of aging at 433 K, whereas the solute depletion mechanism caused by the grain boundary precipitation followed thereafter. The simulation model taking into account such a vacancy depletion effect well reproduced the obtained experimental results, suggesting that the difference of size distribution of Cu clusters after quenching is responsible for the initial formation of PFZ in the subsequent aging stage.

(Received January 17, 2005; Accepted May 2, 2005; Published June 15, 2005)

Keywords: *precipitate free zones, aluminum-copper alloy, grain boundary, phase decomposition, Guinier-Preston zones, transmission electron microscopy, computer simulation, Monte Carlo method*

1. Introduction

Precipitate free zones (PFZ) in the vicinity of grain boundaries have been recognized to possess detrimental effects on mechanical and electrochemical properties of age-hardenable aluminum alloys. Two mechanisms are widely accepted to account for the formation of PFZ from the viewpoint of either vacancy depletion or solute depletion. The vacancy depletion mechanism[1–3] takes into account the effects of vacancy sinks during quenching, resulting in the retarded precipitation around grain boundaries compared with that inside grains. Under the solute depletion mechanism,[4] on the other hand, the suppressed precipitation adjacent to grain boundaries is attributed to the decreased supersaturation of solute atoms, which is frequently induced in conjunction with the formation of more stable and coarsened grain boundary precipitates. Experimental approach to verify the solute depletion mechanism seems to be easier because microchemical analysis by using energy dispersive X-ray spectroscopy (EDX) and energy filtering transmission electron microscopy (EFTEM) is available these days. On the other hand, vacancy depletion is hardly detected through any conventional techniques, and therefore computational investigation becomes a method to inquire into the atomistic behaviors of vacancies, as well as solute atoms, during the formation of PFZ. Hirosawa *et al.*[5–9] developed a lattice Monte Carlo model with vacancy mechanism to reproduce the phase decomposition of various aluminum alloys and low-alloy steels. Their atomic-scale simulation successfully provided useful information about movement of diffusing atoms and vacancies, nucleation and growth of precipitates, segregation of alloying elements and so on.

In this work, the formation mechanism of PFZ has been experimentally clarified for a quenched and artificially aged Al–1.74 mol%Cu alloy at 433 K using TEM and EDX. To reveal the atomistic behaviors of Cu atoms and vacancies, furthermore, a simulation model taking into account the effects of vacancy sinks was also established by improving our previously developed Monte Carlo model.[5–9] The comparison between the experimental and computational results suggests that PFZ is formed not only by the suppressed diffusion of Cu atoms due to the depletion of vacancies but also by the competition between dissolution and growth of Cu clusters at the moderate aging temperatures.

2. Experimental Investigation by TEM and EDX

2.1 Experimental procedures

An Al–1.74 mol%Cu alloy was fabricated from high-purity elemental ingots. The homogenized, hot- and cold-rolled sheets were solution-treated at 793 K for 3.6 ks, followed by iced-water quenching. The subsequent aging treatment was carried out at 433 K for various aging times. The foils for TEM observation were prepared by a twin-jet polishing technique in a solution of 20 vol% nitric-acid and 80 vol% methanol at ~250 K. TEM observation was performed only for high-angle grain boundaries with contact angles of $>10^\circ$, which are generally accepted to exhibit wider width of PFZ than that of low-angle grain boundaries,[4] using a JEM 3010 transmission electron microscope at an accelerating voltage of 300 kV. EDX analysis to estimate residual Cu concentrations within the α-Al matrix was carried out across grain boundaries with a small electron beam of ~15 nm in probe size.

2.2 Experimental results

Figure 1(a) illustrates a typical TEM micrograph showing the existence of PFZ along a grain boundary of the under-aged alloy. The precipitates inside grains have been identified to be plate-like Guinier-Preston zones (hereafter GP zones) with an average size of ~15 nm. It is also seen in Fig. 1(a) that the number density of GP zones is smaller at the edge of PFZ than that within grains. The corresponding EDX profile revealed that Cu concentration is highly maintained at

*Graduate student, Tokyo Institute of Technology.
Present address: Sumitomo Light Metal Industries, Ltd., 3-1-12 Chitose, Minato-ku, Nagoya 455-8670, Japan

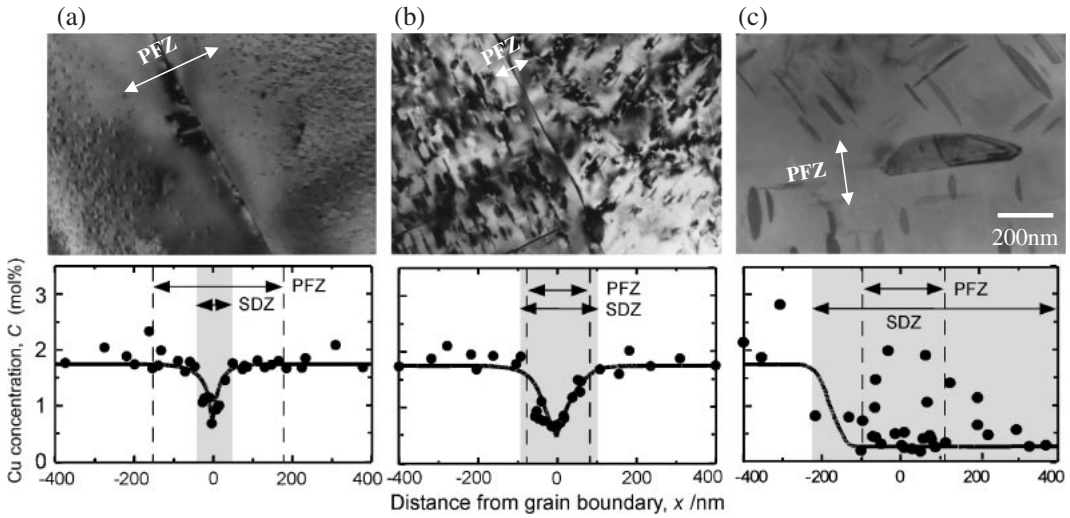

Fig. 1 TEM micrographs and EDX profiles around grain boundaries of the Al–Cu alloy aged at 433 K for 7.2 ks (under-aged) (a), 90 ks (peak-aged) (b) and 1728 ks (over-aged) (c). The average widths of precipitate free zone (PFZ) and solute depletion zone (SDZ) are also indicated by arrows.

~1.7 mol% within PFZ, except in the region adjacent to the grain boundary (In this work, this region is designated as solute depleted zone (SDZ)). Similar supersaturation of solute atoms within PFZ has been reported for Al–Zn–Mg[10–12] and Al–Mg[13] alloys, suggesting that the vacancy depletion mechanism works for the formation of PFZ in various aluminum alloys.

On the other hand, the solute depletion mechanism starts to work predominantly in the later stage of aging. Figure 1(b) and (c) shows TEM micrographs and EDX profiles of the same alloy under the peak-aged and over-aged conditions. Although the precipitates inside grains had changed to GP(2) zones and/or the θ'-Al_2Cu phase, it was found that the decrease in Cu concentrations within PFZ becomes remarkable corresponding to the growth of grain boundary precipitates. This exchange of formation mechanisms can be clearly seen in Fig. 2, where aging time dependence of widths of PFZ and SDZ is represented simultaneously. It is obvious that the width of PFZ decreases in the early stage of aging and then gradually increases with aging time, whereas SDZ monotonously increases in width, thus giving rise to the identical width with that of PFZ at ~30 ks. Similar change of the width of PFZ has been observed in Al–Zn–Mg alloys.[12,14] From the experimental results, therefore, PFZ was found to be formed by the combination of the two mechanisms if the alloys are quenched and aged at moderate temperatures. Note that high aging temperatures only increase the width of PFZ due to the faster formation of grain boundary precipitates.[4,15]

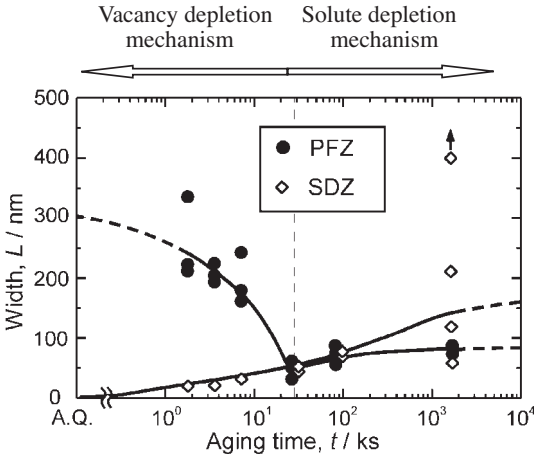

Fig. 2 Time dependence of widths of precipitate free zone (PFZ) and solute depleted zone (SDZ) in the artificially aged Al–Cu alloy at 433 K.

3. Computational Investigation by Monte Carlo Simulation

3.1 Simulation model and parameters

A newly established simulation model taking into account the vacancy depletion mechanism is based on our previously developed Monte Carlo model.[5–9] Three rigid face-centered cubic lattices with $50 \times 50 \times 100$ unit cells (total lattice sites: one million) were set up normal to a grain boundary and designated in sequence as Region A, B and C [Fig. 3(a)]. The initial configurations of atoms and vacancies in the three regions were generated by randomly distributed Al, Cu and vacancies with the same composition as experimentally utilized Al–1.74 mol%Cu. In this model, a series of simulations was performed under a simplified procedure of heat treatments in Fig. 3(b), where continuous cooling from a solution treatment temperature, T_s, and up-quenching to an aging temperature, T_a, are assumed to occur instantly without changing microstructures. Therefore, the effects of vacancy sinks during quenching were taken into account only as the difference of vacancy concentrations during holding at a quenching temperature, T_q; *i.e.* ${C_v}^A$, ${C_v}^B$ and ${C_v}^C$ (${C_v}^A < {C_v}^B < {C_v}^C$) depending on the distance from the grain boundary [Fig. 3(c)]. Note that the same vacancy concentration of ${C_v}^A$ was allocated to the three regions when simulating the subsequent aging treatment at T_a. The actual procedure of the exchange between an atom and a vacancy under the periodic boundary condition is described elsewhere.[5–9]

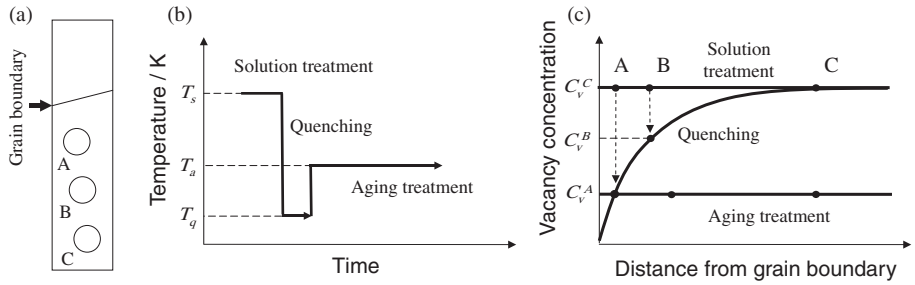

Fig. 3 Schematic illustrations of the locations of three regions A, B and C (a), a simplified procedure of heat treatments (b) and assumed vacancy concentrations at the regions (c) utilized in the present simulation model.

The utilized interaction parameter between Al and Cu, $V_{Al\text{-}Cu}$, was derived under the regular solution approximation;

$$V_{Al\text{-}Cu} = RT[\ln(1-c) - \ln c]/[z(1-2c)], \qquad (1)$$

where R is the gas constant, T the temperature at a copper content c and z the coordination number. It should be noted that our estimated $V_{Al\text{-}Cu} = 1303\,\mathrm{J/mol}$ by using the values of GP zone solvus $T_{sol} = 450\,\mathrm{K}$ at $c = 0.0174$ provides a symmetrical miscibility gap (dotted line) well closely along by the reported GP zone solvus[16] (dashed line) as illustrated in Fig. 4. Therefore, Al-Cu binary system had been regarded as a good example of our simulations involving phase separation because coherent GP zones consisting of condensed Cu atoms form within the dilute α-Al matrix.

As for the interaction parameter between Cu and vacancy, on the other hand, slightly repulsive force of $V_{Cu\text{-}v} = 860$ J/mol was utilized as previously estimated from known thermodynamic parameters.[5–7] This is in agreement with an experimental knowledge that Cu atoms have no significant vacancy trapping effect in aluminum alloys.

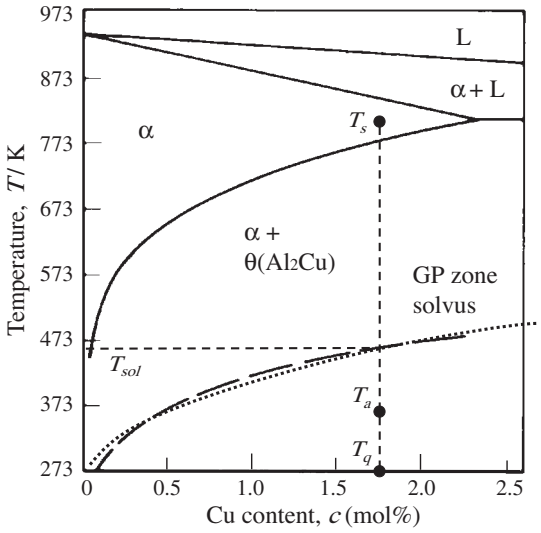

Fig. 4 Equilibrium phase diagram of Al–Cu system (solid lines) with the reported GP zone solvus[16] (dashed line). A miscibility gap (dotted line) was assumed under the regular solution approximation for the present simulation model.

3.2 Simulation results

Figure 5 illustrates the simulated evolution of Cu clusters in Regions A to C of the Al–Cu alloy held at T_q and then aged at T_a. The values of T_q and T_a were assumed to be $0.61T_{sol}$ and $0.72T_{sol}$ because the experimentally applied aging temperature of $0.96T_{sol}$ was too high to reach the metastable microstructures within practically performable simulation times. Note that the experimental trends at 433 K could be maintained at lower aging temperatures although the detection of GP zones, and therefore PFZ, becomes much difficult.

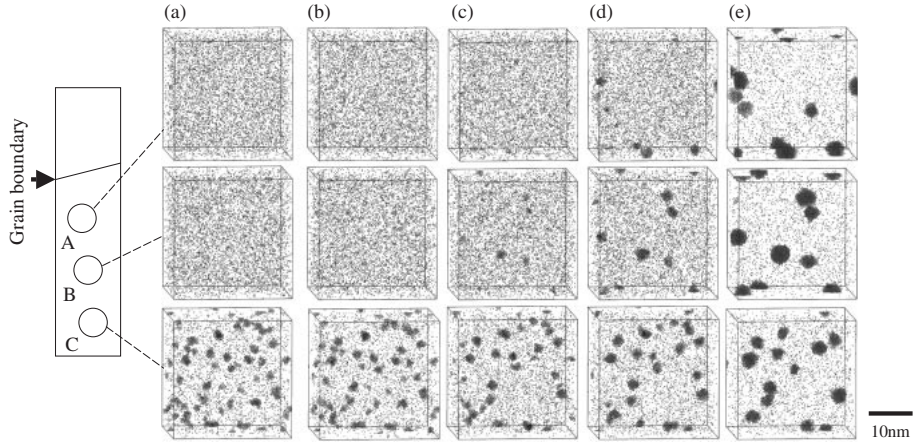

Fig. 5 Simulated evolution of Cu clusters in Regions A to C of the Al–Cu alloy. Only Cu atoms are depicted by black dots after held at T_q for 1×10^7 MCS (a), and then aged at T_a for 1×10^9 MCS (b), 1×10^{10} MCS (c), 2×10^{10} MCS (d) and 1×10^{11} MCS (e). Here, MCS (Monte Carlo Step) is a computational unit indicating the total number of attempts for a vacancy to exchange the positions with a neighboring atom.

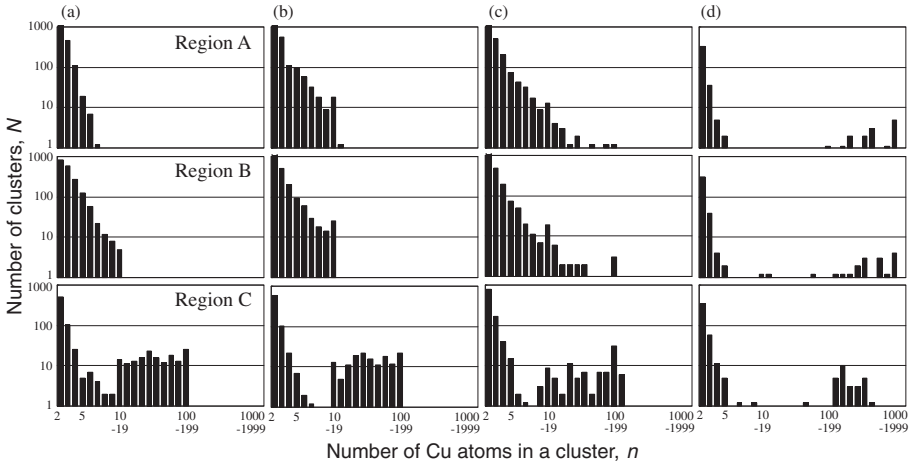

Fig. 6 Size distribution of Cu clusters in Regions A to C of the simulated Al–Cu alloy held at T_q for 1×10^7 MCS (a), and then aged at T_a for 1×10^9 MCS (b), 1×10^{10} MCS (c) and 1×10^{11} MCS (d). The corresponding snapshots of the simulation microstructures are illustrated in Fig. 5.

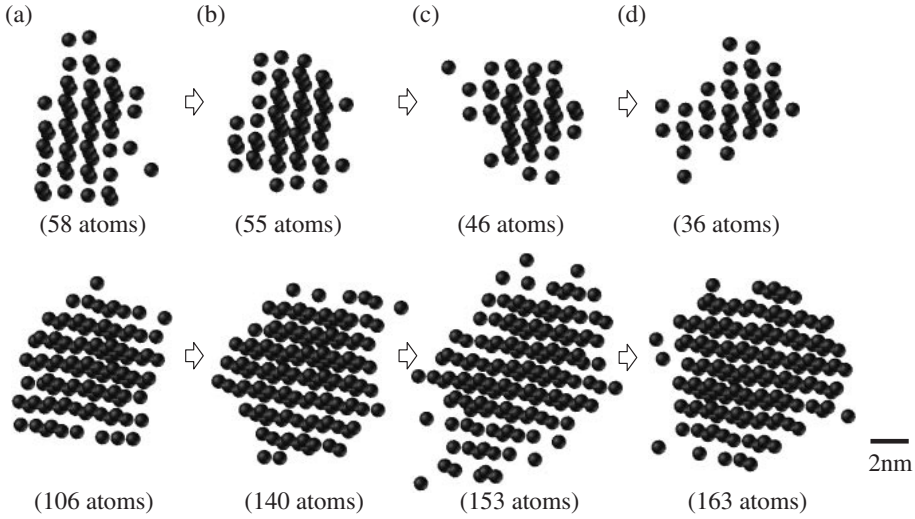

Fig. 7 Dynamic evolution of Cu clusters in Regions C of the simulated Al–Cu alloy during aging at T_a. (a) 0 MCS (after holding at T_q), (b) 1×10^9 MCS, (c) 2×10^9 MCS (c) and (d) 5×10^9 MCS.

As a result of microstructural changes at T_q, the different configurations of Cu atoms were formed; *i.e.* the suppressed clustering of Cu in Region A as opposed to the formation of well-defined Cu clusters in Region C [Fig. 5(a)]. This difference of microstructures after quenching was simply induced by the different vacancy concentrations of ${C_v}^A = 10^{-6}$, ${C_v}^B = 10^{-5}$ and ${C_v}^C = 10^{-4}$, therefore the mobility of Cu atoms was found to be crucial in determining the degree of microstructural development from the initially generated random distributions.

Under the subsequent aging treatment, furthermore, quite interesting characteristics on the evolution of Cu clusters were observed in our simulation model. From a series of simulation snapshots in Fig. 5, for example, Regions A could be recognized to be within PFZ at 1×10^{10} MCS [Fig. 5(c)], but after prolonged simulation steps larger Cu clusters were formed with a lower number density than those in Regions B and C [Fig. 5(d), (e)]. This is quantitatively revealed in Fig. 6, where the size distribution of Cu clusters in Regions A, B and C is illustrated as a function of MCS. The suppressed formation of Cu clusters in Region A resulted in the sparsely distributed Cu clusters with lager cluster sizes over 1000 Cu atoms, whereas initially developed Cu clusters in Region C, but still beyond the resolution limit of TEM, kept the high number density even after 1×10^{11} MCS. These simulation results are in good agreement with the experimentally obtained ones; *i.e.* the continuous decrease in width of PFZ and the formation of larger and sparsely distributed precipitates at the edge of PFZ. Figure 7 illustrates the enlarged snapshots of Cu atom configurations at a fixed position within Region C. Smaller Cu clusters after quenching exhibit a tendency to dissolve at T_a, whereas larger ones to grow steadily, resulting in the higher number dencity of precipitates. Such an atomistic behavior of Cu atoms is only revealed by well-established simulation models. Note that a few computational approaches have been attempted on the formation mechanism of PFZ by Jiang and Faulkner[17,18] and Okuda and Ochiai.[19–21]

4. Conclusions

In this work, the formation mechanism of PFZ has been experimentally clarified for a quenched and artificially aged Al–1.74 mol%Cu alloy using TEM and EDX. From the detailed microstructural and microchemical analysis, it was found that the exchange of principal mechanisms takes place during aging at 433 K from the vacancy depletion mechanism to the solute depletion mechanism. Our newly developed Monte Carlo model taking into account the effects of vacancy sinks revealed that the distribution of precipitates after prolonged aging times is attributed to the microstructural changes occurring during quenching. From a series of simulations, it was suggested that PFZ is formed not only by the suppressed diffusion of Cu atoms around grain boundaries but also by the competition between dissolution and growth of Cu clusters at the aging temperatures. The present simulation model qualitatively well reproduced the experimentally obtained results; *i.e.* the continuous decrease in width of PFZ and the formation of larger and sparsely distributed precipitates at the edge of PFZ. However, the effect of elastic strain would be a subject of further investigation by our simulation model to overcome the morphological disagreement between spherical and plate-like precipitates.

Acknowledgements

This study has been conducted as “Nanotechnology Metal Project” supported by New Energy and Industrial Technology Development Organization (NEDO) and The Japan Research and Development Center for Metals (JRCM). Generous financial assistance from The Light Metal Educational Foundation, Inc. is also gratefully appreciated.

REFERENCES

1) J. L. Taylor: J. Inst. Metals **92** (1963–64) 301.
2) J. D. Embury and R. B. Nicholson: Acta Metall. **13** (1965) 403–417.
3) G. W. Lorimer and R. B. Nicholson: Acta Metall. **14** (1966) 1009–1013.
4) A. J. Cornish and M. K. B. Day: J. Inst. Metals **97** (1969) 44–52.
5) S. Hirosawa, T. Sato, J. Yokota and A. Kamio: Mater. Trans. JIM **39** (1998) 139–146.
6) S. Hirosawa, T. Sato, A. Kamio and H. M. Flower: Acta Mater. **48** (2000) 1797–1806.
7) S. Hirosawa and T. Sato: Modelling Simul. Mater. Sci. Eng. **9** (2001) 129–141.
8) A. Cerezo, S. Hirosawa, I. Rozdilsky and G. D. W. Smith: Philos. Trans. R. Soc. London, Ser. A **361** (2003), 463–477.
9) S. Hirosawa and T. Sato: J. Japan Inst. of Light Metals **54** (2004) 121–127.
10) P. Doig, J. W. Edington and G. Hibbert: Philos. Mag. **28** (1973) 971–981.
11) M. Raghavan, Metall. Trans. A **11** (1980) 993–999.
12) S. Hirosawa, Y. Oguri, T. Ogura and T. Sato: Proc. 9th Int. Conf. on Aluminum Alloys, (Inst. of Mater. Eng. Australia Ltd, 2004) pp. 666–671.
13) H. Yukawa, Y. Murata, M. Morinaga, Y. Takahashi and H. Yoshida: Acta Mater. **43** (1995) 681–688.
14) M. Abe, K. Asano and A. Fujiwara: J. Japan Inst. Metals **36** (1972) 597–604.
15) C. H. Jon, K. Yamada and Y. Miura: Mater. Sci. Forum **331–337** (2000) 1037–1042.
16) G. Lorimer: *Precipitation Processes in Solids*, (The Metallurgical Society of AIME, 1987) pp. 87.
17) H. Jiang and R.G. Faulkner: Acta Mater. **44** (1996) 1857–1864.
18) H. Jiang and R. G. Faulkner: Acta Mater. **44** (1996) 1865–1871.
19) H. Okuda and S. Ochiai: Mater. Trans. **45** (2004) 1455–1460.
20) H. Okuda and S. Ochiai: Proc. 9th Int. Conf. on Aluminum Alloys, (Inst. of Mater. Eng. Australia Ltd, 2004) pp. 152–157.
21) H. Okuda and S. Ochiai: Mater. Sci. Forum **475–479** (2005) 937–940.